Chapter 12

Applications

In this chapter, we describe how to put deep learning models to practical use. We begin by discussing the large scale neural network implementations required for most serious AI applications. Next, we review several specific application areas that deep learning has been used to solve. While one goal of deep learning is to design algorithms that are capable of solving a broad variety of tasks, so far some degree of specialization is needed. For example, vision tasks require processing a large number of input features (pixels) per example. Language tasks require modeling a large number of possible values (words in the vocabulary) per input feature.

12.1 Large Scale Deep Learning

Deep learning is based on the philosophy of connectionism: while an individual biological neuron or an individual feature in a machine learning model is not intelligent, a large population of these neurons or features acting together can exhibit intelligent behavior. It truly is important to emphasize the fact that the number of neurons must be *large*. One of the key factors responsible for the improvement in neural network's accuracy and the improvement of the complexity of tasks they can solve between the 1980s and today is the dramatic increase in the size of the networks we use. As we saw in Chapter 1.2.3, network sizes have grown exponentially for the past three decades, yet artificial neural networks are only as large as the nervous systems of insects.

Because the size of neural networks is of paramount importance, deep learning requires high performance hardware and software infrastructure.

12.1.1 Fast CPU Implementations

Traditionally, neural networks were trained using the CPU of a single machine. Today, this approach is generally considered insufficient. We now mostly use GPU computing or the CPUs of many machines networked together. Before moving to these expensive setups, researchers worked hard to demonstrate that CPUs could not manage the high computational workload required by neural networks.

A description of how to implement efficient numerical CPU code is beyond the scope of this book, but we emphasize here that careful implementation for specific CPU families can yield large improvements. For example, in 2011, the best CPUs available could run neural network workloads faster when using fixed-point arithmetic rather than floating-point arithmetic. By creating a carefully tuned fixed-point implementation, Vanhoucke *et al.* (2011) obtained a 3× speedup over a strong floating-point system. Each new model of CPU has different performance characteristics, so sometimes floating-point implementations can be faster too. The important principle is that careful specialization of numerical computation routines can yield a large payoff. Other strategies, besides choosing whether to use fixed or floating point, including optimizing data structures to avoid cache misses and using vector instructions. Many machine learning researchers neglect these implementation details, but when they restrict the size of the network one can train, they in turn restrict the machine learning capabilities of the network.

12.1.2 GPU Implementations

Most modern neural network implementations are based on graphics processing units. Graphics processing units (GPUs) are specialized hardware components that were originally developed for graphics applications. The consumer market for video gaming systems spurred development of graphics processing hardware. The performance characteristics needed for good video gaming systems turn out to be beneficial for neural networks as well.

Video game rendering requires performing many operations in parallel quickly. Models of characters and environments are specified in terms of lists of 3-D coordinates of vertices. Graphics cards must perform matrix multiplication and division on many vertices in parallel to convert these 3-D coordinates into 2-D on-screen coordinates. The graphics card must then perform many computations at each pixel in parallel to determine the color of each pixel. In both cases, the computations are fairly simple and do not involving much branching compared to the computational workload that a CPU usually encounters. For example, each vertex in the same rigid object will be multiplied by the same matrix; there is no need to evaluate an if statement per-vertex to determine which matrix to multiply by. The computations are also entirely independent of each other, and thus may be parallelized easily. The computations also involve processing massive buffers of memory, containing bitmaps describing the texture (color pattern) of each object to be rendered. Together, this results in graphics cards having been designed to have a high degree of parallelism and high memory bandwidth, at the cost of having a lower clock speed and less branching capability relative to traditional CPUs.

Neural networks also benefit from the same performance characteristics. Neural networks usually involve large and numerous buffers of parameters, activation values, and gradient values, each of which must be completely updated during every step of training. These buffers are large enough to fall outside the cache of a traditional desktop computer so the memory bandwidth of the system often becomes the rate limiting factor. GPUs offer a compelling advantage over CPUs due to their high memory bandwidth. Neural network training algorithms typically do not involve much branching or sophisticated control, so they are appropriate for neural network hardware. Since neural networks can be divided into multiple individual "neurons" that can be processed independently from the other neurons in the same layer, neural networks easily benefit from the parallelism of GPU computing.

GPU hardware was originally so specialized that it could only be used for graphics tasks. Over time, GPU hardware became more flexible, allowing custom subroutines to be used to transform the coordinates of vertices or assign colors to pixels. In principle, there was no requirement that these pixel values actually be based on a rendering task. These GPUs could be used for scientific computing by writing the output of a computation to a buffer of pixel values. Steinkrau *et al.* (2005) implemented a two-layer fully connected neural network on an early GPU and reported a 3X speedup over their CPU-based baseline. Shortly thereafter, Chellapilla *et al.* (2006) demonstrated that the same technique could be used to accelerate supervised convolutional networks.

The popularity of graphics cards for neural network training exploded after the advent of *General Purpose GPUs*. These GP-GPUs could execute arbitrary code, not just rendering subroutines. NVIDIA's CUDA programming language provided a way to write this arbitrary code in a C-like language. With their relatively convenient programming model, massive parallelism, and high memory bandwidth, GP-GPUs now offer an ideal platform for neural network programming. This platform was rapidly adopted by deep learning researchers soon after it became available (Raina *et al.*, 2009; Ciresan *et al.*, 2010).

Writing efficient code for GP-GPUs remains a difficult task best left to specialists. The techniques required to obtain good performance on GPU are very different from those used on CPU. For example, good CPU-based code is usually designed to read information from the cache as much as possible. On GPU, most writable memory locations are not cached, so it can actually be faster to compute the same value twice, rather than compute it once and read it back from memory. GPU code is also inherently multi-threaded and the different threads must be coordinated with each other carefully. For example, memory operations are faster if they can be *coalesced*. Coalesced reads or writes occur when several threads can each read or write a value that they need simultaneously, as part of a single memory transaction. Different models of GPUs are able to coalesce different kinds of read or write patterns. Typically, memory operations are easier to coalesce if among n threads, thread i accesses byte $i + j$ of memory, and j is a multiple of some power of 2. The exact specifications differ between models of GPU. Another common consideration for GPUs is making sure that each thread in a group executes the same instruction simultaneously. This means that branching can be difficult on GPU. Threads are divided into small groups called *warps*. Each thread in a warp executes the same instruction during each cycle, so if different threads within the same warp need to execute different code paths, these different code paths must be traversed sequentially rather than in parallel.

Due to the difficulty of writing high performance GPU code, researchers should structure their workflow to avoid needing to write new GPU code in order to test new models or algorithms. Typically, one can do this by building a software library of high performance operations like convolution and matrix multiplication, then specifying models in terms of calls to this library of operations. For example, the machine learning library Pylearn2 (Warde-Farley *et al.*, 2011) specifies all of its machine learning algorithms in terms of calls to the Theano (Bergstra *et al.*, 2010a; Bastien *et al.*, 2012) and cuda-convnet (Krizhevsky, 2010), which provide these high-performance operations. This factored approach can also ease support for multiple kinds of hardware. For example, the same Theano program can run on either CPU or GPU, without needing to change any of the calls to Theano itself. Other libraries like Torch (Collobert *et al.*, 2011b) provide similar features.

12.1.3 Large Scale Distributed Implementations

In many cases, the computational resources available on a single machine are insufficient. We therefore want to distribute the workload of training and inference across many machines.

Distributing inference is simple, because each input example we want to process can be run by a separate machine. This is known as *data parallelism*.

It is also possible to get *model parallelism*, where multiple machines work together on a single datapoint, with each machine running a different part of the model. This is feasible for both inference and training.

Data parallelism during training is somewhat harder. We can increase the size of the minibatch used for a single SGD, but usually we get less than linear returns in terms of optimization performance. It would be better to allow multiple machines to compute multiple gradient descent steps in parallel. Unfortunately, the standard defintion of gradient descent is as a completely sequential algorithm: the gradient at step t is a function of the parameters produced by step $t - 1$.

This can be solved using *asynchronous stochastic gradient descent* (Bengio *et al.*, 2001a; Recht *et al.*, 2011). In this approach, several processor cores share the memory representing the parameters. Each core reads parameters without a lock, then computes a gradient, then increments the parameters without a lock. This reduces the average amount of improvement that each gradient descent step yields, because some of the cores overwrite each other's progress, but the increased rate of production of steps causes the learning process to be faster overall. Dean *et al.* (2012) pioneered the multi-machine implementation of this lock-free approach to gradient descent, where the parameters are managed by a *parameter server* rather than stored in shared memory. Distributed asynchronous gradient descent remains the primary strategy for training large deep networks and is used by most major deep learning groups in industry (Chilimbi *et al.*, 2014; Wu *et al.*, 2015). Academic deep learning researchers typically cannot afford the same scale of distributed learning systems but some research has focused on how to build distributed networks with relatively low-cost hardware available in the university setting (Coates *et al.*, 2013).

12.1.4 Model Compression

In many commercial applications, it is much more important that the time and memory cost of running inference in a machine learning model be low than that the time and memory cost of training be low. For applications that do not require personalization, it is possible to train a model once, then deploy it to be used by billions of users. In many cases, the end user is more resource-constrained than the developer. For example, one might train a speech recognition network with a powerful computer cluster, then deploy it on mobile phones.

A key strategy for reducing the cost of inference is *model compression* (Buciluǎ *et al.*, 2006). The basic idea of model compression is to replace the original, expensive model with a smaller model that requires less resources to store and evaluate.

Model compression is applicable when the size of the original model is driven primarily by a need to prevent overfitting. In most cases, the model with the lowest generalization error is an ensemble of several independently trained models. Evaluating all n ensemble members is expensive. Sometimes, even a single model generalizes better if it is large (for example, if it is regularized with dropout).

These large models learn some function $f(\boldsymbol{x})$, but do so using many more parameters than are necessary for the task. Their size is necessary only due to the limited number of training examples. As soon as we have fit this function $f(\boldsymbol{x})$, we can generate a training set containing infinitely many examples, simply by applying f to randomly sampled points $\boldsymbol{x}$. We then train the new, smaller, model to match $f(\boldsymbol{x})$ on these points. In order to most efficiently use the capacity of the new, small model, it is best to sample the new $\boldsymbol{x}$ points from a distribution resembling the actual test inputs that will be supplied to the model later. This can be done by corrupting training examples or by drawing points from a generative model trained on the original training set.

Alternatively, one can train the smaller model only on the original training points, but train it to copy other features of the model, such as its posterior distribution over the incorrect classes (Hinton *et al.*, 2014).

12.1.5 Dynamic Structure

One strategy for accelerating data processing systems in general is to build systems that have *dynamic structure* in the graph describing the computation needed to process an input. Data processing systems can dynamically determine which subset of many neural networks should be run on a given input. Individual neural networks can also exhibit dynamic structure internally by determining which subset of features to compute given information from the input. This form of dynamic structure inside neural networks is sometimes called *conditional computation* (Bengio, 2013a; Bengio *et al.*, 2013a) , though many kinds of dynamic structure predate this term. Since many components of the architecture may be relevant only for a small amount of possible inputs, the system can run faster by computing these features only when they are needed.

Dynamic structure of computations is a basic computer science principle applied generally throughout the software engineering discipline. The simplest versions of dynamic structure applied to neural networks are based on determining which subset of some group of neural networks (or other machine learning models) should be applied to a particular input.

A venerable strategy for accelerating inference in a classifier is to use a *cascade* of classifiers. The basic idea is that we are trying to detect the presence of a rare object (or event). To know for sure that the object is present, we must use a sophisticated classifier with high capacity, that is expensive to run. However, because the object is rare, we can usually reject inputs as not containing the object with much less computation. In these situations, we can train a sequence of classifiers. The first classifiers in the sequence have low capacity, and are trained to have high recall. In other words, they are trained to make sure we do not wrongly reject an input when the object is present. The final classifier is trained to have high precision. At test time, we run inference by running the classifiers in a sequence, abandoning any example as soon as any one element in the cascade rejects it. Overall, this allows us to verify the presence of objects with high confidence, using a high capacity model, but does not force us to pay the cost of inference in a high capacity model for every example. The system as a whole has somewhat high capacity just from the use of many models, even if all of the individual models have the same capacity. It is also possible to design the cascade so that models that come later have higher capacity. Viola and Jones (2001) used a cascade of boosted decision trees to implement a fast and robust face detector suitable for use in handheld digital cameras. Their classifier localizes a face using essentially a sliding window approach in which many windows are examined and rejected if they do not contain faces. Another version of cascades uses the earlier models to implement a sort of hard attention mechanism, e.g. with early members of the cascade localizing an object and later members of the cascade performing further processing on it. For example, Google transcribes address numbers from Street View imagery using a two-step cascade that first locates the address number with one machine learning model and then transcribes it with another (Goodfellow *et al.*, 2014d).

Decision trees themselves are an example of dynamic structure, because each node in the tree determines which of its subtrees should be evaluated for each input. A simple way to accomplish the union of deep learning and dynamic structure is to train a decision tree in which each node uses a neural network to make the splitting decision (Guo and Gelfand, 1992), though this has typically not been done with the primary goal of accelerating inference computations.

TODO–cite work on hard mixtures of experts TODO–work on attention mechanisms, Olshausen's dynamic routing

One major obstacle to using dynamically structured systems is the decreased degree of parallelism that results from the system following different code branches for different inputs. This means that few operations in the network can be described as matrix multiplication or batch convolution on a minibatch of examples. We can write more specialized sub-routines that convolve each example with different kernels or multiply each row of a design matrix by a different set of columns of weights. Unfortunately, these more specialized subroutines are difficult to implement efficiently. CPU implementations will be slow due to the lack of cache coherence and GPU implementations will be slow due to the lack of coalesced memory transactions and the need to serialize warps when members of a warp take different branches. In some cases, these issues can be mitigated by partitioning the examples into groups that all take the same branch, and processing these groups of examples simultaneously. This can be an acceptable strategy for minimizing the time required to process a fixed amount of examples in an offline setting. In a real-time setting where examples must be processed continuously, partitioning the workload can result in load-balancing issues. For example, if we assign one machine to process the first step in a cascade and another machine to process the last step in a cascade, then the first will tend to be overloaded and the last will tend to be underloaded. Similar issues arise if each machine is assigned to implement different nodes of a neural decision tree.

12.1.6 Specialized Hardward Implementations of Deep Networks

Since the early days of neural networks research, hardware designers have worked on specialized hardware implementations that could speed up training and/or inference of neural network algorithms. See early and more recent reviews of specialized hardware for deep networks (Lindsey and Lindblad, 1994; Beiu *et al.*, 2003; Misra and Saha, 2010).

Different forms of specialized hardware (Graf and Jackel, 1989; Mead and Ismail, 2012; Kim *et al.*, 2009; **?**; Chen *et al.*, 2014a,b) have been considered over the last decades, starting with ASICs (application-specific integrated circuit), either with digital (based on binary representations of numbers), analog (Graf and Jackel, 1989; Mead and Ismail, 2012) (based on physical implementations of continuous values as voltages or currents) or hybrid implementations (combining digital and analog components), and in recent years with the more flexible FPGA (field programmable gated array) implementations (where the particulars of the circuit can be written on the chip after it has been built).

Whereas software implementations on general-purpose processing units (CPUs and GPUs) typically use 32 or 64 bits precision floating point representations of numbers, it has long been known that it was possible to use less precision, at least at inference time (Holt and Baker, 1991; Holi and Hwang, 1993; Presley and Haggard, 1994; Simard and Graf, 1994; Wawrzynek *et al.*, 1996; Savich *et al.*, 2007). This has become a more pressing issue in recent years as deep learning has gained in popularity in industrial products, and as the great impact of faster hardware was demonstrated with GPUs. Another factor that motivates current research on specialized hardware for deep networks is that the rate of progress of a single CPU or GPU core has slowed down, and most recent improvements in computing speed have come from parallelization across cores (either in CPUs or GPUs). This is very different from the situation of the 1990's (the previous neural network era) where the hardware implementations of neural networks (which might take two years from inception to availability of a chip) could not keep up with the rapid progress and low prices of general-purpose CPUs. Building specialized hardware is thus a way to push the envelope further, at a time when new hardware designs are being developed for low-power devices such as phones, aiming for general-public applications of deep learning (e.g., with speech, computer vision or natural language).

Recent work on low-precision implementations of backprop-based neural nets

(Vanhoucke *et al.*, 2011; Courbariaux *et al.*, 2015; Gupta *et al.*, 2015) suggests that between 8 and 16 bits of precision can suffice for using or training deep neural networks with back-propagation. What is clear is that more precision is required during training than at inference time, and that some forms of dynamic fixed point representation of numbers can be used to reduce how many bits are required per number. Whereas fixed point numbers are restricted to a fixed range (which corresponds to a given exponent in a floating point representation), dynamic fixed point representations share that range among a set of numbers (such as all the weights in one layer). Using fixed point rather than floating point representations and using less bits per number reduces the surface area, power requirements and computing time needed for performing multiplications, and multiplications are the most demanding of the operations needed to use or train a modern deep network with backprop.

12.2 Computer Vision

Computer vision has traditionally been one of the most active research areas for deep learning applications. Many of the most popular standard benchmark tasks for deep learning algorithms are forms of object recognition or optical character recognition.

Computer vision is a very broad field encompassing a wide variety of ways of processing images, and an amazing diversity of applications such as recovering sound waves from the vibrations they induce in objects visible in a video (Davis *et al.*, 2014). Most deep learning research on computer vision has not focused on such exotic applications that expand the realm of what is possible with imagery but rather a small core of AI goals aimed at replicating human abilities. Most deep learning for computer vision is used for object recognition or detection of some form, whether this means reporting which object is present in an image, annotating an image with bounding boxes around each object, transcribing a sequence of symbols from an image, or labeling each pixel in an image with the identity of the object it belongs to. Because generative modeling has been a guiding principle of deep learning research, there is also a large body of work on image synthesis using deep models. While image synthesis *ex nihilo* is usually not considered a computer vision endeavor, models capable of image synthesis are usally useful for image restoration, a computer vision task involving repairing defects in images or removing objects from images.

12.2.1 Preprocessing

Many application areas require sophisticated preprocessing because the original input comes in a form that is difficult for many deep learning architectures to represent. Computer vision usually requires relatively little of this kind of preprocessing. The images should be standardized so that their pixels all lie in the same, reasonable range, like [0,1] or [-1, 1]. Mixing images that lie in [0,1] with images that lie in [0, 255] will usually result in failure. This is the only kind of preprocessing that is strictly necessary. Many computer vision architectures require images of a standard size, so images must be cropped or scaled to fit that size. However, even this rescaling is not always strictly necessary. some convolutional models are able to process variable size input if their output varies in size with the input or if they use Some convolutional models accept variably-sized inputs and dynamically adjust the size of their pooling regions to keep the output size constant (Waibel *et al.*, 1989). Other convolutional models have variable-sized output that automatically scales in size with the input, such as models that denoise or label each pixel in an image (Hadsell *et al.*, 2007).

Many other kinds of preprocessing are less necessary but help to reduce the size of the model required to obtain good accuracy on the training set, the amount of time required for training, or the size of the training set required to obtain good accuracy on the test set.

Any form of preprocessing that removes some of the complexity from the vision task will accomplish both of these goals. Simpler tasks do not require as large of models to solve, and simpler solutions are more likely to generalize well. Preprocessing of this kind is usually designed to remove some kind of variability in the input data that is easy for a human designer to describe and that the human designer is confident has no relevance to the task. When training with large datasets and large models, this kind of preprocessing is often unnecessary, and it is best to just let the model learn which kinds of variability it should become invariant to. For example, the AlexNet system for classifying ImageNet only has one preprocessing step: subtracting the mean across training examples of each pixel (Krizhevsky *et al.*, 2012a).

Another approach to preprocessing is to artificially introduce more variation into the training set. *Dataset augmentation* gives the model more training data without requiring the collection of as much real data. This kind of preprocessing usually increases the optimal model size and the amount of time required for training.

Contrast Normalization

One of the most obvious sources of variation that can be safely removed for many tasks is the amount of contrast in the image. Contrast simply refers to the magnitude of the difference between the bright and the dark pixels in an image. There are many ways of quantifying the contrast of an image. In the context of deep learning, contrast usually refers to the standard deviation of the pixels in an image or region of an image. Suupose we have an image represented by a tensor $\mathbf{X} \in \mathbb{R}^{r\times c\times 3}$, with $X_{i,j,0}$ being the red intensity at row i and column j, $X_{i,j,1}$ giving the green intensity and $X_{i,j,2}$ giving the green intensity. Then the contrast of the entire image is given by

$$\sqrt{\frac{1}{3rc}\sum_{i=1}^{r}\sum_{j=1}^{c}\sum_{k=1}^{3}\left(X_{i,j,k}-\bar{\mathbf{X}}\right)^2}$$

where $\bar{\mathbf{X}}$ is the mean intensity of the entire image:

$$\bar{\mathbf{X}} = \frac{1}{3rc}\sum_{i=1}^{r}\sum_{j=1}^{c}\sum_{k=1}^{3}X_{i,j,k}.$$

Global contrast normalization (GCN) aims to prevent images from having varying amounts of contrast by subtracting the mean from each image, then rescaling it so that the standard deviation across its pixels is equal to some constant s. This approach is complicated by the fact that no scaling factor can change the contrast of a zero-contrast image (one whose pixels all have equal intensity). Images with very low but non-zero contrast often have little information content. Dividing by the true stand deviation usually accomplishes nothing more than amplifying sensor noise or compression artifacts in such cases. This motivates introducing a small, positive regularization parameter λ to bias the estimate of the standard deviation. Alternately, one can constrain the denominator to be at least ϵ. Given an input image $\mathbf{X}$, GCN produces an output image $\mathbf{X}'$, defined such that

$$X'_{i,j,k} = s\frac{X_{i,j,k} - \bar{X}}{\max\left\{\epsilon, \sqrt{\lambda + \frac{1}{3rc}\sum_{i=1}^{r}\sum_{j=1}^{c}\sum_{k=1}^{3}\left(x_{i,j,k}-\bar{X}\right)^2}\right\}}. \tag{12.1}$$

Datasets consisting of large images cropped to interesting objects are unlikely to contain any images with nearly constant intensity. In these cases, it is safe to practically ignore the small denominator problem by setting $\lambda = 0$ and avoid division by 0 in extremely rare cases by setting ϵ to an extremely low value like 10^{-8}. This is the approach used by Goodfellow *et al.* (2013a) on the CIFAR-10 dataset. Small images cropped randomly are more likely to have nearly constant intensity, making aggressive regularization more useful. Coates *et al.* (2011) used $\epsilon = 0$ and $\lambda = 10$ on small, randomly selected patches drawn from CIFAR-10.

The scale parameter s can usually be set to 1, as done by Coates *et al.* (2011), or chosen to make each individual pixel have standard deviation across examples close to 1, as done by Goodfellow *et al.* (2013a).

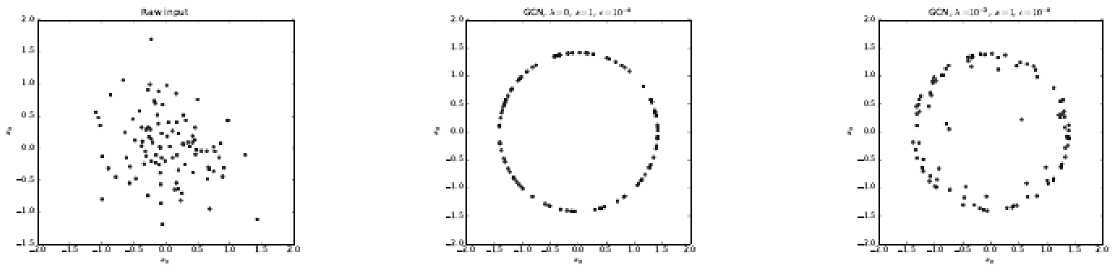

Figure 12.1: GCN maps examples onto a sphere. *Left)* Raw input data may have any norm. *Center)* GCN with $\lambda = 0$ maps all non-zero examples perfectly onto a sphere. *Right)* Regularized GCN, with $\lambda > 0$, draws examples toward the sphere but does not completely discard the variation in their norm.

Note that the standard deviation in equation 12.1 is just a rescaling of the L^2 norm of the image. It is preferable to define GCN in terms of standard deviation so that the same s may be used regardless of image size. However, this observation can be useful because it helps to understand GCN as mapping examples to a spherical shell. See Fig. 12.1 for an illustration. This can be a useful property because neural networks are often better at responding to directions in space rather than exact locations. Responding to multiple distances in the same direction requires hidden units with collinear weight vectors but different biases. Such coordination can be difficult for the learning algorithm to discover. Additionally, many shallow graphical models have problems with representing multiple separated modes along the same line. GCN avoids these problems by reducing each example to a direction rather than a direction and a distance.

Counterintuitively, there is a preprocessing operation known as *sphering* and it is not the same operation as GCN. Sphering does not refer to making the data lie on a spherical shell, but rather to rescaling the principal components to have equal variance, so that the multivariate normal distribution used by PCA has spherical contours. Sphering is more commonly known as *whitening* and is described in section 12.2.1.

Global contrast normalization will often fail to highlight image features we would like to stand out, such as edges and corners. If we have a scene with a large dark area and a large bright area (such as a city square with half the image in the shadow of a building) then global contrast normalization will ensure there is a large difference between the brightness of the dark area and the brightness of the light area. It will not, however, ensure that edges within the dark region stand out.

This motivates *local contrast normalization*. Local contrast normalization ensures that the contrast is normalized across each small window, rather than over the image as a whole. See Fig. 12.2 for a comparison of global and local

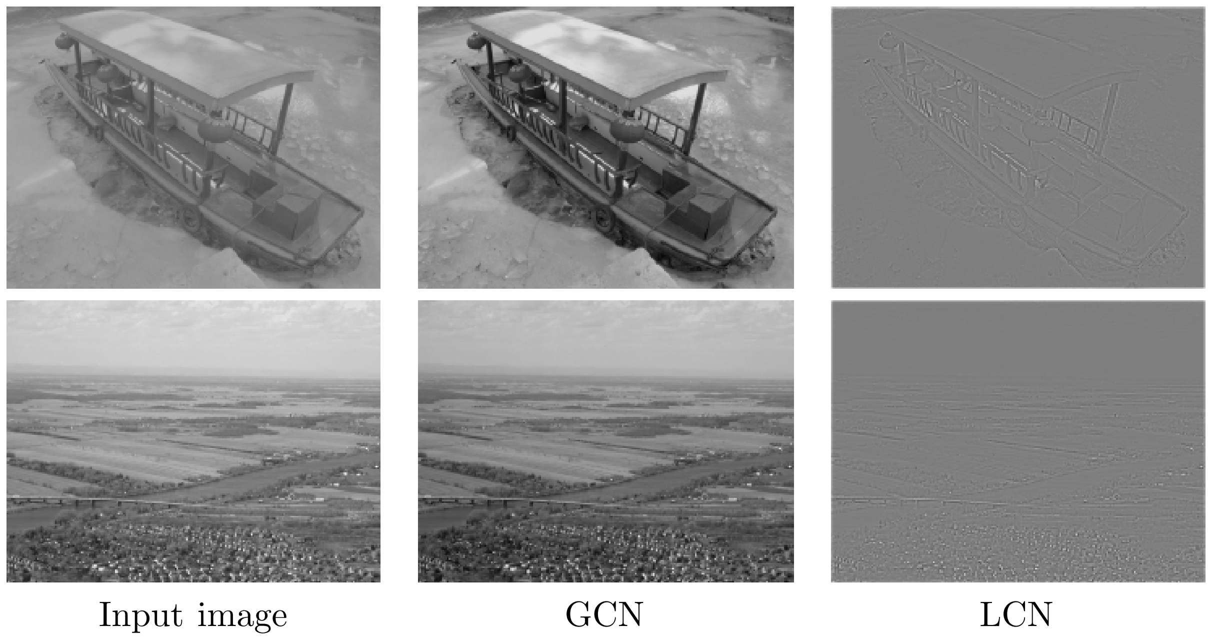

Figure 12.2: A comparison of global and local contrast normalization. Visually, the effects of global contrast normalization are subtle. It places all images on roughly the same scale, which reduces the burden on the learning algorithm to handle multiple scales. Local contrast normalization modifies the image much more, discarding all regions of constant intensity. This allows the model to focus on just the edges. Regions of fine texture, such as the houses in the second row, may lose some detail due to the bandwidth of the normalization kernel being too high.

contrast normalization.

Various definitions of local contrast normalization are possible. In all cases, one modifies each pixel by subtracting a mean of nearby pixels and dividing by a standard deviation of nearby pixels. In some cases, this is literally the mean and standard deviation of all pixels in a rectangular window centered on the pixel to be modified (Pinto *et al.*, 2008). In other cases, this is a weighted mean and weighted standard deviation using Gaussian weights centered on the pixel to be modified. In the case of color images, some strategies process different color channels separately while others combine information from different channels to normalize each pixel (Sermanet *et al.*, 2012).

Local contrast normalization can usually be implemented efficiently by using separable convolution (see Sec. 9.9) to compute feature maps of local means and local standard deviations, then using elementwise subtraction and elementwise division on different feature maps.

Local contrast normalization is a differentiable operation and can also be used as a nonlinearity applied to the hidden layers of a network, as well as a preprocessing operation applied to the input.

As with global contrast normalization, we typically need to regularize local contrast normalization to avoid division by zero. In fact, because local contrast normalization typically acts on smaller windows, it is even more important to regularize. Smaller windows are more likely to contain values that are all nearly the same as each other, and thus more likely to have zero standard deviation.

Whitening

TODO– ZCA and PCA whitening

TODO– refer to Fig. 12.3

TODO–show whitened images: finish figure below

We often regularize ZCA or PCA by adding a small constant to all of the estimated eigenvalues. This is equivalent to adding the same constant to the diagonal of the estimated covariance, i.e., it is equivalent to fitting the covariance matrix to a larger dataset formed by adding isotropric noise to the training examples. It is also common to simply cut out some of the highest frequency components, because these usually correspond to artifacts of the imaging process (Olshausen and Field, 1997).

TODO– convolutional version

Whitening may also be motivated from a biological point of view. Retinal ganglion cells seem to implement a kind of whitening filter. This suggests that when we want to build a model of the lower levels of visual processing in the brain, we should preprocess the input to this model by whitening it, in order to

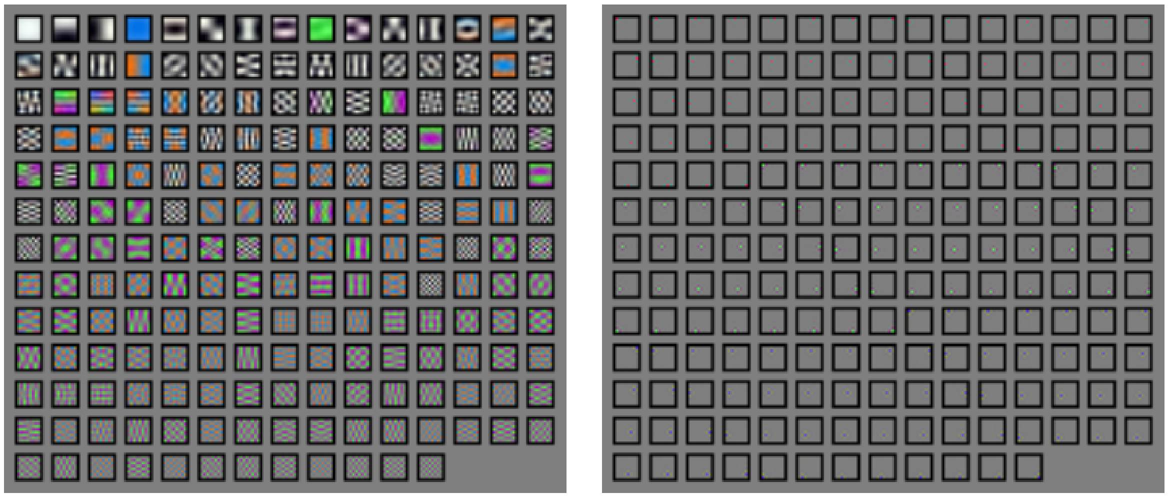

Figure 12.3: The filters learned by PCA and ZCA whitening applied to 8 × 8 pixel patches of the CIFAR-10 dataset. *Left)* PCA filters, arranged left to right, top to bottom. The first filters correspond to the directions of greatest variance. The earliest filters are thus low frequency and the last filters are high frequency. When we apply the PCA transformation, the result is no longer an image with any spatial relationships between the features. *Right)* ZCA filters. Each ZCA filter extracts a center-surround sharpened red, green, or blue pixel. Because the features are all localized in the same way, transforming by the ZCA filters preserves the concept of spatial locality.

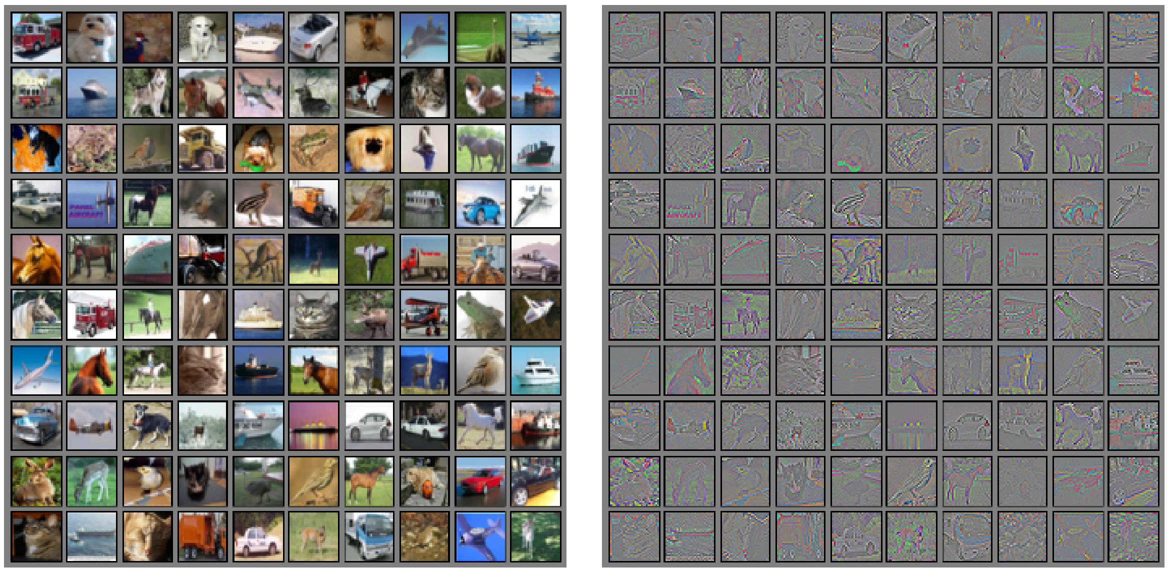

most closely mimic the input provided to the brain from the retina (Olshausen and Field, 1997).

Dataset Augmentation

TODO–random translations, horizontal flips, distortions, color changes (coordinate with regularization chapter)

12.2.2 Convolutional Nets

TODO–Describe how conv nets are usually resource intensive, need good GPU implementation or distributed implementation Cuda-Convnet Pylearn2 + Theano Torch Decaf / Caffe OverFeat DistBelief TODO– Schmidhuber convolutional nets for contests, MNIST TODO– ImageNet TODO– Christian's detection net TODO– Ouais's text transcription HMM TODO– Street Number transcriber TODO– pixel labeling TODO– image restoration

12.3 Speech Recognition

The task of speech recognition consists in mapping an acoustic signal corresponding to a spoken natural language utterance into the corresponding sequence of words intended by the speaker. If we denote by $\boldsymbol{X} = (\boldsymbol{x}_1, \boldsymbol{x}_2, \ldots \boldsymbol{x}_T)$ the input sequence of acoustic vectors (describing the recorded sounds in discrete time units such as the traditional 20ms frames), and by $\boldsymbol{y} = (y_1, y_2, \ldots y_N)$ the target output or linguistic sequence (e.g., whose elements are words or characters from a natural language), the Automatic Speech Recognition (ASR) task can be described as looking for a function $f_{\text{ASR}} \approx f^*_{\text{ASR}}$, where f^*_{ASR} finds the most likely linguistic sequence $\boldsymbol{y}$ given the acoustic sequence $\boldsymbol{X}$:

$$f^*_{\text{ASR}}(\boldsymbol{X}) = \arg\max_{\boldsymbol{y}} P^*(\mathbf{y} | \mathbf{X} = \boldsymbol{X}) \tag{12.2}$$

where P^* is the true conditional distribution relating the inputs $\boldsymbol{X}$ to the targets $\boldsymbol{y}$.

12.3.1 Historical Perspective

Speech recognition was one of the first areas to which neural networks were applied in the 80's and 90's (Bourlard and Wellekens, 1989; Waibel *et al.*, 1989; Robinson and Fallside, 1991; Bengio *et al.*, 1991, 1992b; Konig *et al.*, 1996) and it reached the state-of-the-art that was then (and until recently) held by systems based on Hidden Markov Models (HMMs), which were briefly described in Section 10.9.3 (Rabiner, 1989), along with Gaussian Mixture Models (GMMs) for learning the acoustic density associated with each HMM state. It turned out that with *much larger models*, *deeper models* (more hidden layers), and training with much larget datasets, neural nets could very advantageously replace the GMMs, i.e., basically to associate acoustic features to phonemes (or sub-phonemic states).

Starting in 2009, unsupervised pretraining was used to build stacks of RBMs taking spectral acoustic representations in a fixed-size input window (around a center frame) and predicting the conditional probabilities of HMM states for that center frame. Early results on the TIMIT dataset (the MNIST of speech) suggested that training such deep networks actually helped to significantly improve the HMM recognition rate on TIMIT (Mohamed *et al.*, 2012). This was quickly followed up by work to expand the architecture from phoneme recognition (which is what TIMIT is basically focused on) to large-vocabulary speech recognition (Dahl *et al.*, 2012). By that time, several of the major speech groups in industry had started exploring deep learning (in collaboration with some of the authors of the above papers) for speech recogniton and they collaborated to report on the breakthroughs they were all getting (Hinton *et al.*, 2012a) and these systems started being deployed in products such as Android phones.

As it turned out later, as these groups explored larger and larger labeled datasets and incorporated some of the methods for initializing, training, and setting up the architecture of deep nets, they realized that the unsupervised pretraining phase was either unnecessary or did not bring any significant improvement.

These breakthroughs in recognition performance for speech recognition were unprecedented (around 30% improvement) and were following a long period of about ten years during which error rates did not improve much with the traditional GMM+HMM technology, in spite of the continuously growing size of training sets (see Figure 2.4 of Deng and Yu (2014)). This created a rapid shift in the speech recognition community towards deep learning, at conferences such as ICASSP. In a matter of two years, most of the industrial products for speech recognition incorporated that innovation and this interest spurred a new wave of explorations for deep learning algorithms and architectures, which is still ongoing.

One of these innovations was the use of convolutional networks (Chapter 9) instead of fully-connected feedforward networks (Sainath *et al.*, 2013). In that case the input spectrogram is seen not as one long vector but as an image, with one axis corresponding to time and the other to frequency of spectral components.

Another important push, still ongoing, has been towards end-to-end deep learning speech recognition systems, without the need for the HMM. The first major breakthrough in this direction came from Graves *et al.* (2013) which trained a deep LSTM RNN (see Section 10.8.4), using MAP inference over the frame-to-phoneme alignment, i.e., as in LeCun *et al.* (1998c) and in the the CTC framework (Graves *et al.*, 2006; Graves, 2012), described in more detail in Section 10.9.2. A deep RNN (Graves *et al.*, 2013) has several layers state variables at each time step, making the unfolded graph deep in two ways, ordinary depth due to a stack of layers, and depth due to time unfolding. See Pascanu *et al.* (2014a); Chung *et al.* (2014) for other variants of deep RNNs.

Following that push, the idea was introduced of using an attention mechanism to let the system learn how to "align" the acoustic-level information with the phonetic-level information Chorowski *et al.* (2014).

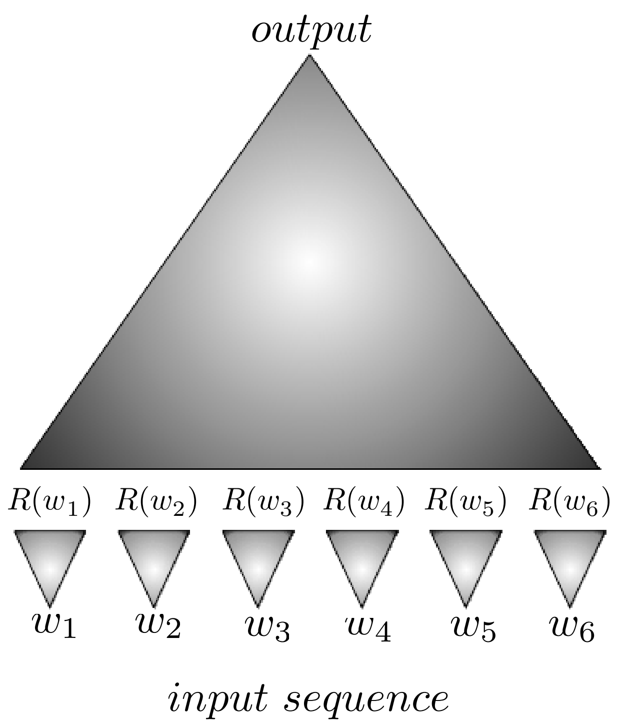
output
$R(w_1)$ $R(w_2)$ $R(w_3)$ $R(w_4)$ $R(w_5)$ $R(w_6)$
w_1 w_2 w_3 w_4 w_5 w_6
input sequence

Figure 12.4: Neural language models and their extensions can always be decomposed into two components: (1) the word embeddings, i.e., a mapping from any word index (a symbol) to a learned vector and (2) other parameters dedicated to the task at hand (such as predicting the next word, or translating one sentence into another), based on those representations. The training objective is defined in terms of the output of the second component. It is the second component that drives the learning of the word embeddings in such a way as to make similar words (according to the task) share attributes or dimensions in their embeddings.

12.4 Natural Language Processing and Neural Language Models

Natural language processing includes applications such as language modeling and machine translation. As with the other applications discussed in this chapter, very generic neural network techniques can be successfully applied to natural language processing. However, to achieve excellent performance and scale well to large applications, some domain-specific strategies become important. Natural language modeling usually forces us to use some of the many techniques that are specialized for processing sequential data. In many case, we choose to regard natural language as a sequence of words, rather than a sequence of individual characters. In this case, because the total number of possible words is so large, we are modeling an extremely high-dimensional and sparse discrete space. Several strategies have been developed to make models of such a space efficient, both in a computational and in a statistical sense.

12.4.1 Historical Perspective

The idea of distributed representations for symbols was introduced by Rumelhart *et al.* (1986a) in one of the first explorations of back-propagation, with symbols corresponding to the identity of family members and the neural network capturing the family relationships between family members, e.g., with examples of the form (Colin, Mother, Victoria). It turned out that the first layer of the neural network learned a representation of each family member, with learned features, e.g. for Colin, representing which family tree Colin was in, what branch of that tree he was in, what generation he was from, etc. One can think of these learned features as a set of attributes and the rest of the neural network computing micro-rules relating these attributes together in order to obtain the desired predictions, e.g., who is the mother of Colin? A similar idea was the basis of the research on neural language model started by Bengio *et al.* (2001b), where this time each symbol represented a word in a natural languge vocabulary, and the task was to predict the next word given a few previous ones. Instead of having a small set of symbols, we have a vocabulary with tens or hundreds of thousands of words (and nowadays it goes up to the million, when considering proper names and misspellings). This raises serious computational challenges, discussed below in Section 12.4.4. The basic idea of a neural language models and their extensions, e.g., for machine translation, is illustrated in Figure 12.4 and a specific instance (which was used by Bengio *et al.* (2001b)) is illustrated in Figure 12.4. Figure 12.4 explains the basic of idea of splitting the model into two parts, one for the word embeddings (mapping symbols to vectors) and one for the task to be performed. Sometimes, different maps can be used, e.g., for input words and output words, as in Figure 12.4, or in neural machine translation models (Section 12.4.6).

Earlier work had looked at modeling sequences of characters in text using neural networks (Miikkulainen and Dyer, 1991; Schmidhuber, 1996), but it turned out that working with word symbols worked better as a language model and, more importantly, immediately yielded *word embeddings*, i.e., interpretable representations of words, as illustrated in Figures 12.6 and 12.7. Actually, these compelling 2-dimensional visualization arose thanks to the the development of the t-SNE algorithm (van der Maaten and Hinton, 2008a) in 2008, and the first visualization of word embeddings was made by Joseph Turian in 2009: these t-SNE visualizations of word embedding quickly became a standard tool to understand the learned word representations, first in talks and then in papers.

The early efforts at training language models typically yielded neural nets that did not beat an n-gram model by themselves, but when adding the probability prediction coming from the neural net and from the n-gram model, one would typically get substantial gains in log-likelihood (Bengio *et al.*, 2003a).

An important development after the demonstration that neural language models could be used to improve upon classical n-gram models in terms of negative log-likelihood (also called perplexity in the language modeling literature) has been the demonstration that these improved language models could yield an improvement in word error rate for state-of-the-art speech recognition systems (Schwenk and Gauvain, 2002, 2005; Schwenk, 2007). The same technique (replacing the n-gram by a combination of n-gram and neural language model) was then used to improve classical statistical machine translation systems (Schwenk *et al.*, 2006; Schwenk, 2010).

More developments of the original model are described in the sections below.

12.4.2 The Problem With n-grams

The basic motivation for neural language models discussed by Bengio *et al.* (2001b, 2003a) is that this approach has the potential to bypass the curse-of-dimensionality issue arising with more classical n-gram approaches. To get a clear understanding of the curse of dimensionality issue in general for machine learning, please refer to Sections 5.12.1 and 16.6. In the case of n-grams, the issue amounts to the exponential growth in the number of discrete contexts to be considered. n-gram models store at least one coefficient (a frequency count, typically) for each one of a set of contexts corresponding to a short subsequence of words. Please refer to Section 10.9.1 for a description of language models based on n-grams. As discussed in that section, in order to properly consider longer contexts (of length $n-1$), n-gram models require exponentially growing memory and training data. In practice, this is mitigated by only considering the *most frequent* sets of longer contexts, but this also means that for less frequent longer contexts, the only form of generalization that is possible comes from ignoring the older part of the context.

There is actually another form of generalization that was introduced to n-grams and that can on the surface approach some of the ideas behind distributed representations. So-called class-based language models (Brown *et al.*, 1992; Ney

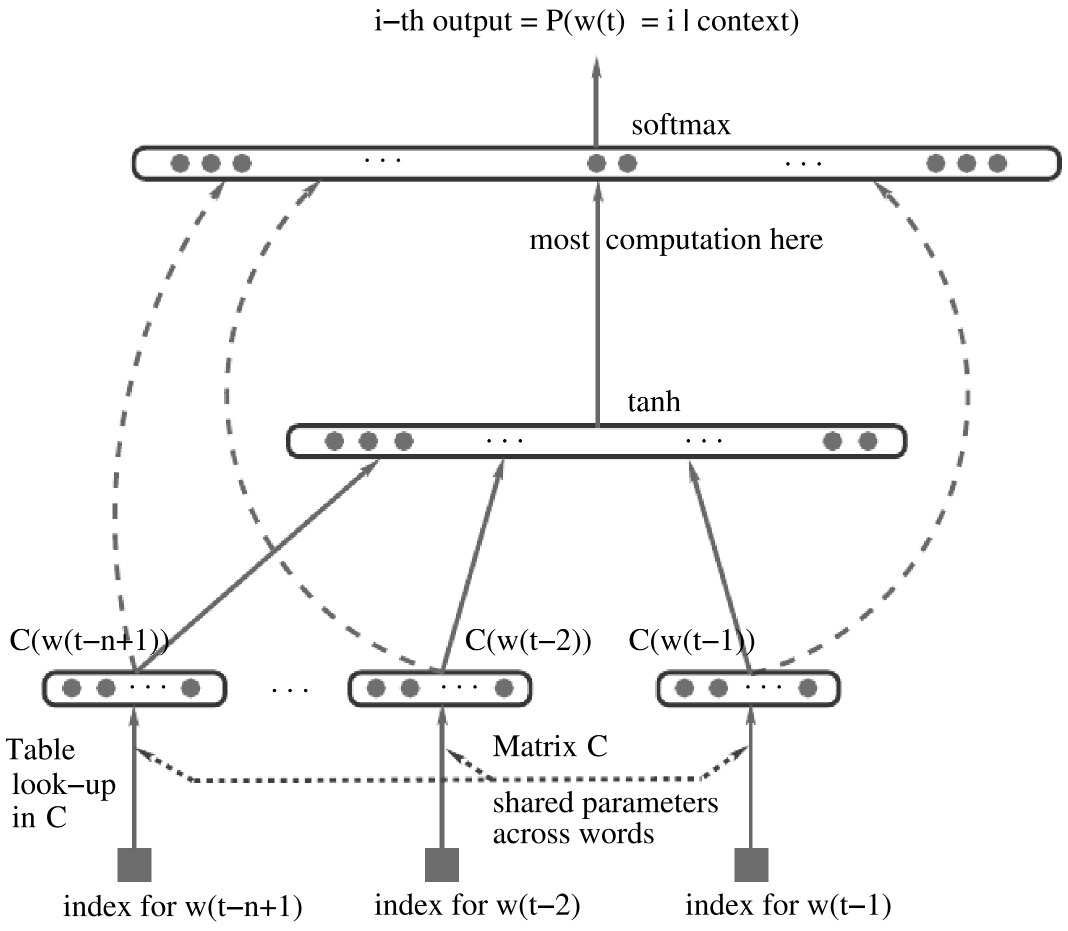

Figure 12.5: This is the original architecture for a neural language model that was developed by Bengio *et al.* (2001b) and is a special case of the general architecture for neural language-related models illustrated in Figure 12.4. Here the "second component" is an ordinary MLP with a single hidden layer and a very large softmax output layer predicting the probability of the next word (given the previous words seen in input).

and Kneser, 1993; Niesler *et al.*, 1998) introduce the notion of word categories in order to share statistical strength between words that are semantically close. The idea is to partition the set of words into clusters or classes (e.g., based on their co-occurence frequencies with other words), and to condition the n-gram probability on a rougher representation than the original tuple of words: the corresponding tuple of word classes. Although this clearly gives a way to generalize between sequences in which some word is replaced by another of the same class, much information is lost in this representation. We can think of the word class as an attribute, but one where the only allowed values are mutually exclusive. If one had multiple attributes (e.g., different ways of partitioning the set of words), then with enough attributes one would get both the benefit of generalization to semantically similar words and the benefit of keeping all the information about the specific choice of word. This is essentially what distributed representations of words (word embeddings) aim to achieve.

12.4.3 How Neural Language Models can Generalize Better

The fundamental reason why neural language models can break the barrier encountered with models based on n-grams is that neural language models can learn an intermediate representation for words, such that there can be a generalization occuring (sharing of statistical strength) between words (and the contexts in which they appear) that have *some* common attributes. For example, if the word `dog` and the word `cat` share many attributes (except maybe some indicator of being feline or not, for example), then sentences that contain the word `cat` can inform the predictions that will be made by the model for sentences that contain the word `dog`, and vice-versa. And because there are many such attributes, there are many ways in which generalization can happen, transfering information from each training sentence to an exponentially large number of semantically related sentences (e.g., in which some words are replaced by semantically similar ones). Basically, the exponential arising in the curse of dimensionality (growing with the sentence size) is addressed with another exponential, arising out of the exponential number of small variations that each element in the sequence can have (and now the exponential grows with the number of dimensions of the representation).

We sometimes call these word representations "word embeddings" because we can think of these representations as points in a semantic space of lower dimension than the raw symbols (which live in a space of dimension equal to the vocabulary size). Whereas in the original space every pair of words is at the same distance as any other pair of words, in the embedding space, semantically similar words (or any pair of words sharing some "features" learned by the model) end up close to each other, and one can also observe different types of words clustering semantically, like shown in Figure 12.6.

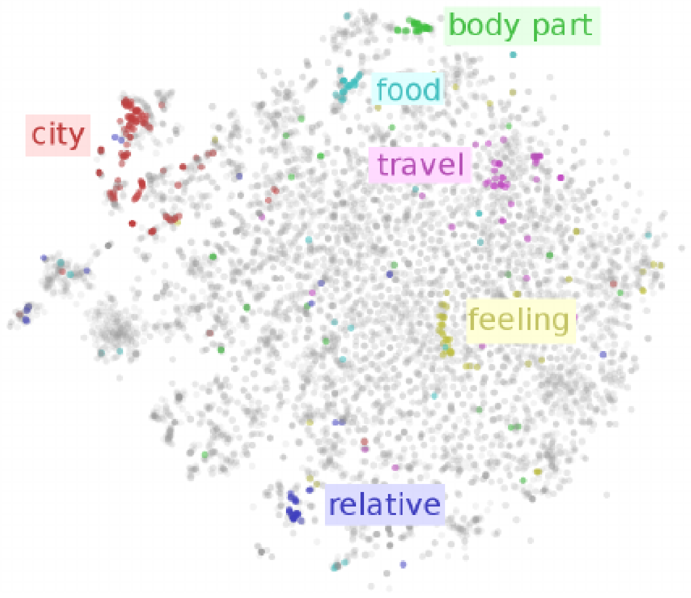

Figure 12.6: Word embeddings obtained from neural language models tend to cluster by semantic categories, as visualized here via t-SNE dimensionality reduction and coloring of words by such categories. Reproduced with permission by Chris Olah from `http://colah.github.io/`, where many more insightful visualizations can be found.

Figure 12.7 zooms in on specific areas of such a picture of word embeddings, and we see more clearly how semantically similar words end up with representations that are close to each other. However, keep in mind that these were obtained using a strong dimensionality reduction (from hundreds to 2), which means that the actual embeddings are much richer than what can be seen via those visualizations.

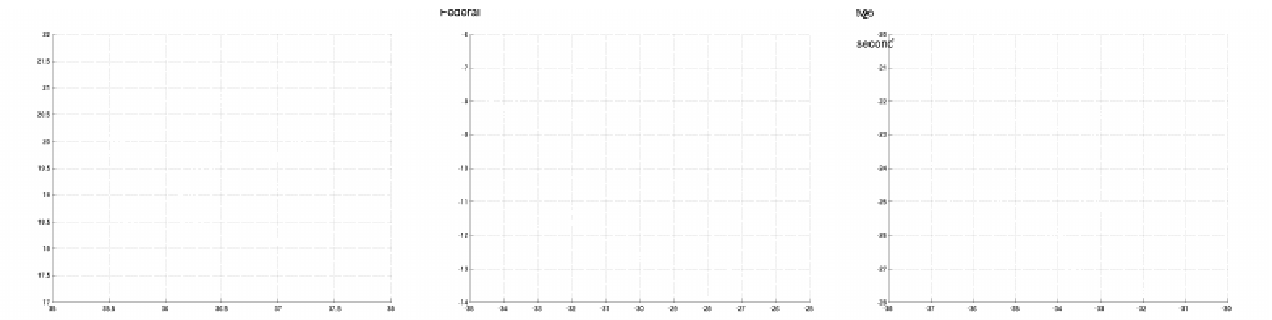

Figure 12.7: Two-dimensional visualizations of word embeddings obtained from a neural machine translation model (Bahdanau *et al.*, 2014), zooming in on specific areas where we see semantically nearby words, e.g., years on the left, countries in the middle, and numbers on the right. Consider Fig. 12.6 for a sense of the big picture.

12.4.4 High-Dimensional Outputs

One of the nagging questions that early work with neural language models raised is the computational cost of the affine/softmax output layer (with one output per word in the vocabulary), both at training time (to compute the likelihood and its gradient) and at test time (to compute probabilities for all or selected words). Indeed, the affine/softmax output layer performs the following computation (see also Section 6.3.1):

$$a_i = b_i + \sum_j W_{ij} h_j \quad \forall i \in \{1, \ldots, |\mathbb{V}|\} \tag{12.3}$$

$$p_i = \frac{e^{a_i}}{\sum_{i' \in \{1,\ldots,|\mathbb{V}|\}} e^{a_{i'}}} \tag{12.4}$$

where $\mathbb{V}$ is the vocabulary and $|\mathbb{V}|$ its size, $\boldsymbol{h}$ is the top hidden layer used to predict the output probabilities $\boldsymbol{p}$, and $\boldsymbol{b}, \boldsymbol{W}$ are learned parameters. If $\boldsymbol{h}$ contains n_h elements then the above operation is $O(|\mathbb{V}| n_h)$. With n_h in the thousand(s) and $|\mathbb{V}|$ in the hundreds of thousands, this computation dominates the computation of most neural language models.

Use of a Short List

The early work dealt with this problem first (Bengio *et al.*, 2003a) by limiting the vocabulary size (e.g. to 10,000 or 20,000 words), then by splitting the vocabulary $\mathbb{V}$ into a short list $\mathbb{L}$ of most frequent words (handled by the neural net) and a tail $\mathbb{T} = \mathbb{V} \backslash \mathbb{L}$ of more rare words (handled by an n-gram model) (Schwenk, 2007). To be able to combine the two predictions, the neural net also has to predict the probability for a word to belong to none of those in the short list. This is achieved by decomposing probabilities as follows:

$$\begin{aligned} P(y = i \mid C) = & 1_{i \in \mathbb{L}} P(y = i \mid C, i \in \mathbb{L}) P(i \in \mathbb{L} \mid C) \\ & + 1_{i \in \mathbb{T}} P(y = i \mid C, i \in \mathbb{T})(1 - P(i \in \mathbb{L} \mid C)) \end{aligned} \tag{12.5}$$

where C stands for the generic context in which we want to predict the next word y, $P(y = i \mid C, i \in \mathbb{L})$ is the usual softmax output of the neural language model, $P(i \in \mathbb{L} \mid C)$ is an extra output of the neural language model (either computed by adding a sigmoid output or simply an extra output to the softmax for the category of words outside of $\mathbb{L}$), and $P(y = i \mid C, i \in \mathbb{T})$ is computed by the n-gram model, normalizing the frequencies only over the output words y that belong to $\mathbb{T}$.

An obvious disadvantage of the short list approach is that the potential generalization advantage of the neural language models is limited to the most frequent words, and this has stimulated the exploration of alternative methods to deal with high-dimensional outputs, described below.

Hierarchical Softmax

When trying to parametrize and compute a multinoulli probability distribution over a large set (e.g. hundreds of thousands of words) of dimension $|\mathbb{V}|$ there is a classical approach (Goodman, 2001) to decompose probabilities hierarchically. Instead of having a number of computations proportional to $|\mathbb{V}|$ (and also proportional to the number of hidden units n_h, in our case), $|\mathbb{V}|$ factor can be reduced to as low as $\log |\mathbb{V}|$. This idea of a hierarchical decomposition of words has been introduced to neural language models by applied by Bengio (2002); Morin and Bengio (2005) and is described below.

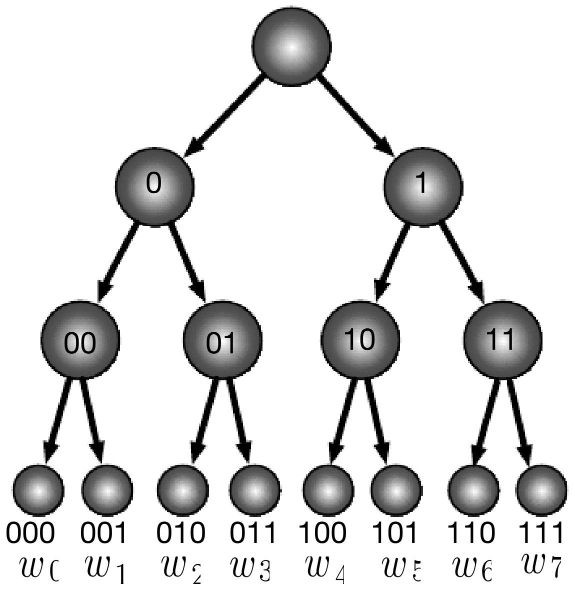

Figure 12.8: Illustration of a hierarchy of word categories, with actual words at the leaves and groups of words at the internal nodes. Any node can be indexed by the sequence of binary decisions (0=left, 1=right) to reach the node from the root. If the tree is sufficiently balanced, the maximum depth (number of binary decisions) is on the order of the logarithm of the number of words $|\mathbb{V}|$: the choice of one out of $|\mathbb{V}|$ words can be obtained by doing $O(\log |\mathbb{V}|)$ operations (one for each of the nodes on the path from the root).

One can think of this hierarchy as corresponding to clusters of categories and cluster of clusters of categories, etc. For example, consider in Figure 12.8 the simple case where we have 8 words $w_0, \ldots, w_7$ organized into a 3-level hierarchy: super-class 0 contains the classes 00 and 01, which respectively contain the words (w_0, w_1) and (w_2, w_3), and similarly super-class 1 contains the classes 10 and 11, which respectively contain the words (w_4, w_5) and (w_6, w_7). Hence, computing the probability of a word y can be done by computing three binomial probabilities, associated with the left or right binary decisions associated with the nodes from the root to a node y. Let b_i be the i-th binary decision when traversing the tree towards the value y. Thus, the probability of sampling and output y can be decomposed into a product of conditional probabilities, using the chain rule for conditional probabilities, with each node indexed by the prefix of these bits, e.g., node 10 in Figure 12.8 corresponds to the prefix $(b_0(w_4) = 1, b_1(w_4) = 0)$, and the probability of w_4 can be decomposed as follows:

$$\begin{aligned} P(\mathrm{y} = w_4) &= P(\mathrm{b}_0 = 1, \mathrm{b}_1 = 0, \mathrm{b}_2 = 0) \\ &= P(\mathrm{b}_0 = 1)P(\mathrm{b}_1 = 0 \mid \mathrm{b}_0 = 1)P(\mathrm{b}_2 = 0 \mid \mathrm{b}_0 = 1, \mathrm{b}_1 = 0). \end{aligned} \tag{12.6}$$

Each of these conditional probabilities can be computed at one node, starting from the root, and associated with the arc going from a parent node to one of its children nodes.

For neural language models, these probabilities are typically conditioned on some context, so in general we decompose the log-likelihood of the next word y given its context as follows:

$$\log P(y \mid C) = \sum_i \log P(b_i \mid b_1, b_2, \ldots, b_{i-1}, C)$$

where the sum runs over all k bits of y. This can be obtained by computing the sigmoid of k dot products, each with a weight vector indexed by the identifier $n = b_1, b_2, \ldots, b_{i-1}$ associated with some internal node n on the path to y:

$$\begin{aligned} p_n &= \mathrm{sigmoid}(c_n + \boldsymbol{v}_n \cdot \boldsymbol{h}_C) \\ \log P(b_i \mid b_1, b_2, \ldots, b_{i-1}, C) &= b_i \log p_n + (1 - b_i)\log(1 - p_n) \end{aligned} \tag{12.7}$$

which corresponds to the usual Bernoulli cross-entropy for logistic regression and probabilistic binary classification in neural networks (Sections 6.3.2 and 6.3.2).

Since the output log-likelihood can be computed efficiently (as low as $\log |\mathbb{V}|$ rather than $|\mathbb{V}|$), so can its gradient with respect to the output parameters (the $\boldsymbol{v}_n$ and c_n above) as well as with respect to the hidden layer activations $\boldsymbol{h}_C$.

Note that in principle we could optimize the tree structure to minimize the expected number of computations, following Shannon's theorem, i.e., by structuring the tree so that the number of bits associated with a word be approximately equal to the logarithm of the frequency of that word. However, in practice, this is typically not worth it because the computation of the output probabilities is only one part of the total computation. For example, if there are several hidden layers of width n_h, then the associated computations grow as $O(n_h^2)$ while the output computations grow as $O(n_h L)$ where L is the average number of bits of output words (weighted by their frequency). Hence, there is not much advantage in making L much less than n_h. Consider that n_h is typically large (e.g., around a thousand or more), and the vocabulary sizes are typically not more than the order of a million. Since $\log_2(10^6)$ is about 20, we could get L on the order of 20 for such a large vocabulary, but in fact it would not make much of a difference to take L on the order of 1000 (the same as n_h), which means that a 2-level tree (which has average depth L on the order of $\sqrt{|\mathbb{V}|}$) is sufficient to reap most of the benefit of a hierarchical softmax, with the typical vocabulary sizes and hidden layer sizes that are currently used. A 2-level tree corresponds to simply defining a set of mutually exclusive words classes.

One question that remains somewhat open is how to best define these word classes, or how to define the word hierarchy in general. Early work used existing hierarchies (Morin and Bengio, 2005) but it can also be learned, ideally jointly with the neural language model, although an exact optimization of the log-likelihood appears intractable because the choice of a word hierarchy is a discrete one, not amenable to gradient-based optimization. However, one could use discrete optimization to approximately optimize the partition of words into word classes.

An important advantage of the hierarchical softmax is that it brings computational benefits both at training time and at test time, if at test time we want to compute the probability of specific words. Of course computing the probability of all $|\mathbb{V}|$ words will remain expensive. Another interesting question is how to pick the most likely word, in a given context, and unfortunately the tree structure does not provide an efficient and exact answer. However, in practice (e.g., for translation or speech recognition), we want to pick the best *sequence* of words, and this typically requires a heuristic search such as the beam search (Section 10.10.1).

A disadvantage is that in practice the hierarchical softmax tends to give worse test results than sampling-based methods such as described below, although this may be due to a poor choice of word classes.

Importance Sampling

An idea that is almost as old as the hierarchical softmax, for speeding up training of neural language models, is the use of a sampling technique to approximate the "negative phase" contribution of the gradient, i.e., the "counter-examples" on which the model should give a low score (or high energy), compared to the observed word. See Section 18.1 for the decomposition of the log-likelihood into a "positive phase" term (pushing the score of the correct word up, or pushing down its energy, which is easy here because we only have to consider one word) and a "negative phase" term (pushing down the score of all the other words, in proportion to the probability that the model gives them). Using the notation introduced in Eq. 12.3, the gradient can be written as follows:

$$
\begin{aligned}
\frac{\partial \log P(y \mid C)}{\partial \theta} &= \frac{\partial \log \operatorname{softmax}_y(\boldsymbol{a})}{\partial \theta} \\
&= \frac{\partial}{\partial \theta} \log \frac{e^{a_y}}{\sum_i e^{a_i}} \\
&= \frac{\partial}{\partial \theta} (a_y - \log \sum_i e^{a_i}) \\
&= \frac{\partial a_y}{\partial \theta} - \sum_i P(i \mid C) \frac{\partial a_i}{\partial \theta})
\end{aligned} \tag{12.8}
$$

where $\boldsymbol{a}$ is the vector of pre-softmax activations (or scores), with one element per word. The first term is the "positive phase" term (pushing a_y up) while the second term is the "negative phase" term (pushing a_i down for all i, with weight $P(i \mid C)$. Since the negative phase term is an expectation, we can estimated by a Monte-Carlo sample. However, that would require sampling from the model itself, i.e., computing $P(i \mid C)$ for all i in the vocabulary, which is precisely what we are trying to avoid.

The solution proposed by Bengio and Sénécal (2003); Bengio and Sénécal (2008) is to sample from another distribution, called the proposal distribution (denoted q), and use appropriate weights to correct for that. This is called *importance sampling* and is introduced in Section 14.1.2. But even exact importance sampling is not appropriate because it requires computing weights p_i/q_i, where $p_i = P(i \mid C)$, which can only be computed if all the scores a_i are computed. The solution adopted is called *biased importance sampling*, where the importance weights are normalized to sum to 1, i.e., when negative word n_i is sampled, the associated gradient is weighted by

$$
w_i = \frac{p_{n_i}/q_{n_i}}{\sum_{j=1}^{N} p_{n_j}/q_{n_j}}.
$$

These weights are used to give the appropriate importance to the N negative samples from q used to form the estimated negative phase contribution to the gradient:

$$
\sum_{i=1}^{|\mathbb{V}|} P(i|C) \frac{\partial a_i}{\partial \theta}) \approx \frac{1}{N} \sum_{i=1}^{N} w_i \frac{\partial a_{n_i}}{\partial \theta}.
$$

In these papers, the authors used a unigram or a bigram distribution as proposal distribution q, because can be easily estimated from the data as well as sampled from very efficiently.

A related application of importance sampling to speed-up training of a larger class of model was introduced by Dauphin *et al.* (2011). These are models where the output is not necessarily a 1-of-n choice (which one can think of as an integer, or as a one-hot vector), but more generally a sparse vector, where only a few of the entries are non-zero. This occurs for example when the output is a *bag-of-words*, i.e., a sparse vector where the non-zeros indicate the presence (0 or 1) or the frequency (a small count) of each word of a document. In the paper, the authors study the case of denoising auto-encoders with a bag-of-words as input. Whereas the sparsity of the input can be easily exploited (by ignoring the zeros in the computation), it is not so clear for the output (reconstruction) units. Because an auto-encoder also predicts its input, the target for the reconstruction is sparse but the prediction (probabilities that any particular word is present) is not. The algorithm ends up minimizing reconstruction error (minus log-likelihood) for the "positive words" (those that are non-zero in the target) and an equal number of "negative words" chosen randomly, but with their gradients reweighted appropriately according to importance sampling.

In all of these cases, the computational complexity of gradient estimation for the output layer is reduced to be proportional to the number of negative samples rather than proportional to the size of the output vector.

Noise-Contrastive Estimation and Ranking Loss

Other approaches based on sampling have been proposed to reduce the computational cost of training neural language models with large vocabularies.

An early one is the ranking loss proposed by Collobert and Weston (2008), in which we view the output of the neural language model for each word as a score and ask that the score of the correct word a_y be ranked high in comparison to the other scores a_i. The ranking loss proposed then is

$$L = \sum_i \max(0, 1 - a_y + a_i). \tag{12.9}$$

Note that the gradient is zero for the i-th term if the score of the observed word, a_y is greater than the score of negative word a_i by a margin of 1. One issue with this criterion is that it does not provide estimated conditional probabilities, which are useful in some applications, e.g., speech recognition, or (conditional) text generation.

A more recently used training objective for neural language model is noise-contrastive estimation, which is introduced in Section 18.6. The idea is to turn the training task into a probabilistic classification problem where the learner tries to identify whether a given value is sampled from the data generating distribution (under the probability estimated by the trained model) or from a fixed "noise" model. This approach has been successfully applied to neural language models (Mnih and Teh, 2012; Mnih and Kavukcuoglu, 2013). That probabilistic classifier output (when the output is the observed word y) can be obtained by combining the score of the observed word a_y with a learned parameter that estimates the log of the normalizing constant of the softmax. The training objective also requires that one samples a word from the "noise" distribution, which acts like a proposal distribution for importance sampling.

12.4.5 Combining Neural Language Models with n-grams to Increase Capacity without Greatly Increasing Computation

A major advantage of n-grams over neural networks is that the computation-capacity trade-off allows n-grams to have a huge capacity (storing all of the frequent tuples frequency) but fast prediction (only looking up a few of those tuples, that match the current context), which almost does not grow with capacity (using hash tables or trees to access the counts). In comparison, doubling a neural network's capacity typically also roughly doubles its computation time[1].

To easily add capacity, it has thus been proposed to combine both approaches, i.e. to use an ensemble consisting of a neural language model and an n-gram language model (Bengio *et al.*, 2001b, 2003a). As with any ensemble, this technique can also reduce test error, and many ways of combining the ensemble members' predictions are possible (uniform weighting, weights chosen on a validation set, etc.) Later, this ensemble idea was extended to include not just two models but a large array of models (Mikolov *et al.*, 2011a) as well as training the neural net jointly with the n-gram model (or rather maximum entropy model) (Mikolov *et al.*, 2011b). Basically, the latter amounts to introducing a very high-dimensional and sparse extra input vector, composed of indicators for the presence of particular n-grams in the input context. In addition, these extra inputs were only connected and directly connected to the outputs. Because these extra inputs are very sparse, the extra computation is minimal, while the added capacity is huge (one parameter for each n-gram tuple considered, i.e., for up to $n-1$ words of context with one output next word).

12.4.6 Neural Machine Translation

The early use of neural networks for machine translation (Schwenk *et al.*, 2006; Schwenk, 2010) took advantage of the good performance of neural language models in order to replace one component of a machine translation system, the statistical language model, which was traditionally done by an n-gram-based model.

[1] it is not true for the word embeddings used in the *input* layer, and the techniques described in Section 12.4.4 allow to reduce computation for the output embeddings, but the capacity added in the intermediate layers still comes with linearly growing computation time.

These n-gram based model include not just traditional back-off n-gram models (Jelinek and Mercer, 1980; Katz, 1987; Chen and Goodman, 1999) but also so-called maximum entropy language models (Berger *et al.*, 1996), in which an affine / softmax layer predicts the next word given the presence of frequent n-grams in the context (as outlined in the previous section).

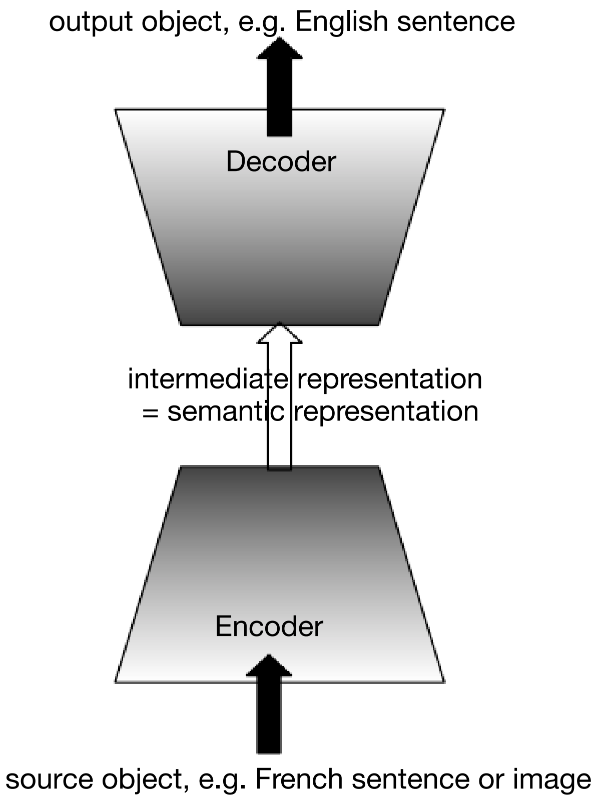
output object, e.g. English sentence
Decoder
intermediate representation
= semantic representation
Encoder
source object, e.g. French sentence or image

Figure 12.9: The encoder-decoder architecture to map back and forth between a surface representation (e.g., sequence of words, image) and a semantic representation. By coupling the encoder for one modality (e.g. French to "meaning") with the decoder for another modality (e.g. "meaning" to English), we can train systems that translate from one modality to another. This idea has been applied successfully not just to machine translation but also to caption generation from images.

However, once we have an architecture for learning neural language model that captures the joint probability $P(\mathrm{w}_1, \mathrm{w}_2, \ldots, \mathrm{w}_T)$ of a sequence of words, we can in principle make the distribution conditional on some generic context C by making some of its parameters a function of C, as explained in Section 6.3.2. For example, Devlin *et al.* (2014) beat the state-of-the-art in some statistical machine translation benchmarks by using an MLP to score a phrase $\mathrm{t}_1, \mathrm{t}_2, \ldots, \mathrm{t}_k$ in the target language given a phrase $\mathrm{s}_1, \mathrm{s}_2, \ldots, \mathrm{s}_n$ in the source language, i.e., estimate $P(\mathrm{t}_1, \mathrm{t}_2, \ldots, \mathrm{t}_k \mid \mathrm{s}_1, \mathrm{s}_2, \ldots, \mathrm{s}_n)$ and use it to replace the traditional phrase table (that estimates the same quantity) based on n-grams. To make this translation more flexible, we would like to use a model that can accommodate variable length inputs and variable length outputs. If an RNN is used to capture $P(\mathrm{w}_1, \mathrm{w}_2, \ldots, \mathrm{w}_T)$, we can make the initial state of the RNN or the biases used at each time step for the hidden units be a function of some generic context C. If C is obtained from a source sentence in another language, we can thus train our neural language to translate from one language to another. If we think of C as a semantic summary of the source sentence, it can for example be obtained as the final state of another RNN (the encoder RNN or "reader"), as in Cho *et al.* (2014); Sutskever *et al.* (2014b); Jean *et al.* (2014), or as the top layer of a convolutional network, as in (Kalchbrenner and Blunsom, 2013). This general idea of an encoder-decoder framework for machine translation is illustrated in Figure 12.9.

This raises the question of representing not just words but sequences of words. The idea of learning a semantic representation of phrases and even sentences so that the representation of the source and target sentences are close to each other and can be mapped from one to the other has been explored (Kalchbrenner and Blunsom, 2013; Cho *et al.*, 2014; Sutskever *et al.*, 2014b; Jean *et al.*, 2014), first using a combination of convolutions and RNNs (Kalchbrenner and Blunsom, 2013) and then using both RNNs for encoding the source sentence and for generating the output target-language sentence (Cho *et al.*, 2014; Sutskever *et al.*, 2014b; Jean *et al.*, 2014).

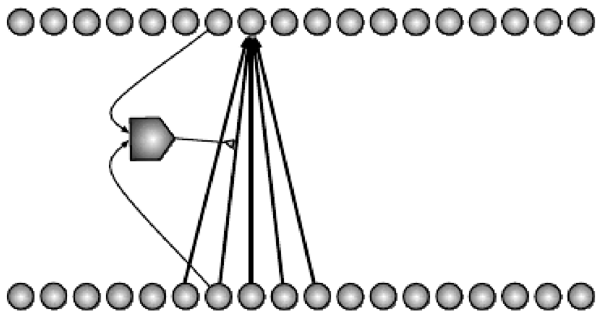

Figure 12.10: Illustration of the attention mechanism used in a neural machine translation system introduced in Bahdanau *et al.* (2014).

Using an Attention Mechanism

Using a fixed-size representation to capture all the semantic details of a very long sentence of say 60 words is very difficult. It can be achieved by training a sufficiently large RNN well enough and for long enough, as demonstrated by Cho *et al.* (2014); Sutskever *et al.* (2014b). However, this is not how humans translate long sequences of words. What they usually do, after having read the whole sentence or paragraph (to get the context and the jist of what is being expressed), they produce the translated words one at a time, each time focusing on a different part of the input sentence in order to gather the semantic details that are required to produce the next output word. That is exactly the idea that Bahdanau *et al.* (2014) first introduced and that is illustrated in Figure 12.10. Earlier work showed that one could learn a kind of translation matrix relating the word embeddings in one language with the word embeddings in another (Kočiský *et al.*, 2014), yielding lower alignmnent error rates than traditional approaches based on the frequency counts in the phrase table. There is even earlier work on learning crosslingual word vectors (Klementiev *et al.*, 2012) and several papers following up on this approach, e.g., to find ways to make crosslingual alignment more efficient (Gouws *et al.*, 2014) to be able to train on larger scale datasets.

12.5 Structured Outputs

In principle, if we have good models $P(\mathbf{Y}|\boldsymbol{\omega})$ of the joint distribution of random variables $\mathbf{Y} = (\mathbf{y}_1, \ldots, \mathbf{y}_k)$, with parameters $\boldsymbol{\omega}$ we can use them to build conditional models $P(\mathbf{Y} \mid \mathbf{X})$ conditioned on some input variables $\mathbf{X}$ by making $\boldsymbol{\omega}$ a parametrized function of the input $\mathbf{X}$. In Chapter 10, in particular with Section 10.4, we saw how an RNN can represent a joint distribution over elements of a sequence that can be conditioned, e.g., on another sequence, such as for machine translation (in the previous section, 12.4.6). Conditional joint distribution models are sometimes called “structured output models”, to distinguish them from the more usual supervised learning tasks where the outputs represent a single random variable (like a class) or conditionally independent random variables (like different attributes, discussed in Section 6.3.2).

In the third part of this book, we will go beyond RNNs as means of capturing the joint distribution between output variables, conditioned on input variables. For example Restricted Boltzmann Machines (RBMs) were made conditional by Taylor *et al.* (2007); Taylor and Hinton (2009) in the context of modeling motion style and by Boulanger-Lewandowski *et al.* (2012) in the context of symbolic sequences describing polyphonic music. In both of these examples, we actually use an RBM as a “output model” for an RNN, i.e., at each time step in the sequence, we want to output a distribution over a group of random variables (articulators for Taylor and Hinton (2009), and musical notes for Boulanger-Lewandowski *et al.* (2012)), given the current state of the RNN. With the RNN-RBM (Boulanger-Lewandowski *et al.*, 2012), a generative model is setup to model a sequence of frames $\boldsymbol{x}_t$, with the following structure. An RNN captures the past context through a state variable $\boldsymbol{h}_t$ that follows a deterministic recurrence

$$\boldsymbol{h}_t = f(\boldsymbol{h}_{t-1}, \boldsymbol{x}_t).$$

In addition, at each time step, a joint distribution over the elements of the next frame $\boldsymbol{x}_{t+1}$ is formed using an RBM with parameters $\boldsymbol{\omega}$:

$$P(\mathbf{x}_{t+1} = \boldsymbol{x}_{t+1} \mid \boldsymbol{\omega}_t).$$

The RBM parameters $\boldsymbol{\omega}_t = (\boldsymbol{\omega}_{\mathrm{RBM}}, \boldsymbol{\omega}'_t)$ are composed of two subsets of parameters, the parameters $\boldsymbol{\omega}_{\mathrm{RBM}}$ that are ordinary parameters (namely the weights of the RBM and the visible units biases) and the parameters $\boldsymbol{\omega}'_t$ that are conditioned on the RNN state $\boldsymbol{h}_t$ (namely, the hidden units biases):

$$\boldsymbol{\omega}'_t = g(\boldsymbol{h}_t).$$

where both f and g have free parameters that are going to be updated by SGD, along with $\boldsymbol{\omega}_{\mathrm{RBM}}$. Since $\boldsymbol{\omega}_t$ is a function of the past frames, we are modeling the joint distribution of the sequence of frames:

$$\begin{aligned} P(\boldsymbol{x}_1, \ldots, \boldsymbol{x}_T) &= \prod_t P(\boldsymbol{x}_{t+1} | \boldsymbol{x}_t, \boldsymbol{x}_{t-1}, \ldots, \boldsymbol{x}_1) \\ &= \prod_t P(\boldsymbol{x}_{t+1} \mid \boldsymbol{\omega}_t) = \prod_t P(\mathbf{x}_{t+1} | \boldsymbol{h}_t). \end{aligned} \tag{12.10}$$

The contrastive divergence algorithm can be used to obtain an estimated log-likelihood gradient on $\boldsymbol{\omega}_t$ in a conditional RBM (Taylor *et al.*, 2007):

$$\delta\boldsymbol{\omega} \approx \frac{\partial \log P(\mathbf{x}_{t+1} = \boldsymbol{x}_{t+1} \mid \boldsymbol{\omega})}{\partial \boldsymbol{\omega}}.$$

Let us decompose δ like $\boldsymbol{\omega}_t$ into $\delta = (\delta_{\mathrm{RBM}}, \delta')$ for the part that corresponds to $\boldsymbol{\omega}_{\mathrm{RBM}}$ and the part that corresponds to $\boldsymbol{\omega}'_t$. The estimated gradient δ_{RBM} can be used to update ω_{RBM} directly (e.g., by SGD) while δ' can be back-propagated through the RNN (as if it was the true gradient of $\log P(\mathbf{x}_{t+1} = \boldsymbol{x}_{t+1} | \boldsymbol{\omega}_t)$ with respect to $\boldsymbol{\omega}'_t$), thereby providing the estimated gradient on the parameters of f and g.

12.6 Other Applications

TODO– dimensionality reduction (nature paper)

TODO– clustering

TODO– collaborative filtering (including Netflix), the explore-exploit issues arising there YOSHUA

TODO– knowledge graphs YOSHUA